Adsorption of Poly(ethylene oxide) at the Air–Solution Interface Studied by Neutron Reflection

A. R. Rennie

Institut Laue-Langevin, 156X, 38042 Grenoble Cedex, France

R. J. Crawford, E. M. Lee, and R. K. Thomas*

Physical Chemistry Laboratory, University of Oxford, South Parks Road, Oxford, OX1 3QZ England

T. L. Crowley and S. Roberts

Department of Chemistry and Applied Chemistry, University of Salford, Salford, England

M. S. Qureshi and R. W. Richards

Department of Pure and Applied Chemistry, University of Strathclyde, Thomas Graham Building, 295 Cathedral Street, Glasgow, G11XL Scotland. *Received September 26, 1988; Revised Manuscript Received January 16, 1989*

ABSTRACT: Specular reflection of neutrons has been used to study the adsorption of poly(ethylene oxide) (PEO) at the air–water interface. This paper describes the reflection technique and its application to the determination of the segment density distribution of polymers as a function of depth. Concentrations between 0.004% and 0.1% by weight PEO in water were studied, as well as the effects of addition of $MgSO_4$ and increasing the temperature to approach the Θ point. Our results indicate that the surface layer has a thickness that is comparable to the radius of gyration in solution and that the segment density in the layer increases with both increasing temperature and increasing concentration. There is, however, always an appreciable quantity of water in the surface region. The surface also appears to be "roughened" on a scale comparable with the effective segment length of the polymer.

Introduction

Two earlier papers have shown how the specular reflection of neutrons may be used to determine the structural properties of adsorbed layers at the air–water interface.[1,2] In this paper we apply the technique to the study of the adsorption of poly(ethylene oxide) at the air–water interface.

There is hardly any direct information available about the configuration of polymers adsorbed at the air–liquid interface, largely because of a lack of suitable experimental techniques. The adsorption of PEO at this interface has been studied by Glass[3] by means of surface tension measurements using the pendant drop technique. He was able to derive adsorption isotherms for different molecular weights and to follow the rate of adsorption of polymer at the interface. Kuzmenka and Granick[4,5] have used a surface balance to determine Π–*A* isotherms of PEO layers on electrolyte solutions and Sauer et al.[6] have also obtained Π–*A* isotherms but using laser light scattering to measure the surface pressure. However, these techniques give no direct structural information about the layer. Experiments that may give more direct information are ellipsometry,[7] X-ray fluorescence,[8] and the specular reflection of X-rays.[9] However, in the first two of these techniques there is not a direct connection between the measured quantities and the interfacial structure. In the third technique it is not usually possible to separate unambiguously the interfacial structure of solute and solvent.

Experimental Section

Neutron Reflectometer. The reflectivity measurements were done on the small-angle scattering spectrometer D17 at the Institut Laue-Langevin, Grenoble.[10] This instrument is designed to examine samples oriented in the vertical plane using a horizontal neutron beam. It had to be modified to study reflection from liquids as shown schematically in Figure 1.

The instrument is on the end of a cold neutron guide. Cadmium slits on each end of the evacuated collimator tube were used to define a beam of height 1.5 mm and width 25 mm. The slits directed the beam onto a multilayer mirror mounted on a Euler cradle at the normal sample position of the instrument. The mirror deflected the beam down on to the liquid surface at a glancing angle. The angle of the mirror with respect to the beam, and hence the angle of incidence of the beam on the liquid sample, could be controlled accurately by rotating it about a horizontal axis perpendicular to the beam. Any neutrons emerging from the sides or the back of the mirror were prevented from reaching the detector by cadmium shielding and further collimation was introduced by an adjustable cadmium knife edge close to the center of the mirror. The multilayer structure of the mirror[11] was chosen to give a uniform reflectivity close to unity up to glancing angles of 0.08 rad (at the liquid surface) for an incident wavelength of 12 Å. The beam reflected from the liquid surface was measured on a BF_3 multidetector consisting of a 128 × 128 array of 5 × 5 mm cells, placed 133 cm from the liquid. The resolution of the experiment was mainly determined by the spread in the incident wavelengths for which $\Delta\lambda/\lambda$ was 10%.

In principle, a measurement of reflectivity as a function of momentum transfer, $\kappa = 4\pi \sin\theta/\lambda$, of the neutron normal to the liquid sample can be done in either of two ways, by varying the incident wavelength at a fixed angle of incidence or by varying the incident angle at a fixed wavelength. The disadvantage of the latter is that at low glancing angles the incident beam has to be severely collimated to prevent illumination of an area larger than that of the sample. At higher angles this leads to a loss of intensity unless the collimating slits can be adjusted correspondingly. Over a series of measurements it may not be possible to do this with sufficient reproducibility. The disadvantage of varying only the wavelength is that the neutron flux is a maximum at 12 Å and therefore at any other wavelength there is a relative reduction in signal. A combination of the two methods was therefore used, reflectivities over the κ range 0.015–0.039 $Å^{-1}$ being done at a fixed incident angle of 2.16° with wavelengths 12.0–31.2 Å, and those in the κ range 0.044–0.062 $Å^{-1}$ at a fixed wavelength of 12 Å and incident angles varying from 2.38° to 3.55°.

The absolute reflectivity at any value of the momentum transfer was determined by two measurements. The liquid surface was lowered so that the beam passed through the sample container windows but above the liquid surface. The intensity and position of this "straight through" beam was measured on the multidetector. The liquid surface was then raised into the reflecting

0024-9297/89/2222-3466$01.50/0

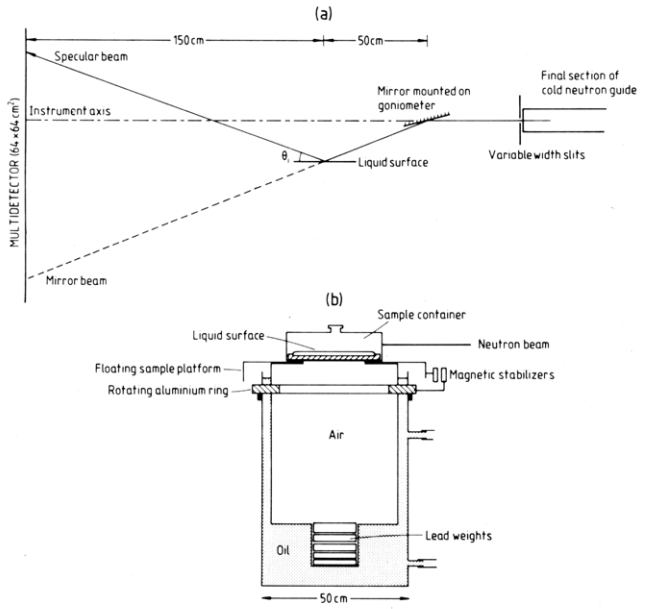

Figure 1. Configuration of the D17 neutron small-angle scattering machine when used for a specular reflection experiment: (a) beam, mirror, and multidetector configuration: (b) the sample mount.

position and the intensity of the reflected beam recorded. After subtraction of the background (see below), the ratio of the intensities obtained in these two measurements gave the absolute reflectivity directly. The angle of the incident beam was calculated from the position of the "straight through" beam on the detector.

Sample Container. The sample was contained in a PTFE trough 5 mm deep with an area of liquid surface 200 × 80 mm^2. The trough was initially cleaned by soaking it for several days in Analar heptane followed by overnight soaking in a mixture of 4% HF in concentrated HNO_3. Finally, it was washed in ultrapure water (Elgastat UHQ, Elga, U.K.). Beteen sample changes the trough and all glassware were cleaned with chromic acid followed by ultrapure water.

The trough was housed in a sealed aluminium container to keep the solution free from contamination and to prevent convective currents arising from evaporation of solvent. The container was carefully masked with cadmium to eliminate all sources of stray scattered neutrons. The temperature of the sample environment was controlled with an absolute accuracy of ±2° by using a specially built controller. This consisted of a Pt resistance thermometer attached to the wall of the container and connected to a battery-operated infrared transmitter. This transmitter switched two externally mounted, infrared heating lamps as needed. To ensure even heating of the sample by these two lamps, the can was shielded by black anodized heat collectors which transmitted heat to the sample by conduction. The whole was enclosed in an outer PMMA container. Both containers had soda glass windows which transmitted about 85% of the incident neutrons. The assembly of the trough and containers was done away from the float system described below to prevent any possible contamination by oil.

The components of the D17 spectrometer are mounted on a metal frame and would transmit much of the ambient vibration to the sample. The effect of this would be to roughen the surface to levels where it could be impossible to interpret reflectivity measurements. To minimize this problem, the sample container was mounted on a platform floating in low vapor pressure oil. The weight of the float (about 40 kg, mostly in the base) and the viscosity of the oil combined to damp out ambient vibrations reasonably effectively.

The liquid surface was aligned accurately by means of a light source, which could be placed in the neutron beam before the final piece of neutron guide. The height of the surface was adjusted by the addition or removal of small volumes of oil from the outer container. A problem that arises with a floating system is that of rotation or drift of the floating platform. This is particularly awkward if, as in this case, the sample is well shielded with cadmium, because parts of the main beam are then obscured. This problem was overcome by means of three mutually repulsive sets of magnets mounted on both floating and stationary parts of the float assembly, which held the floating platform in the center of the outer oil container.

Preparation and Characterization of Polymers. Deuterioethylene oxide monomer was obtained from Merck, Sharpe & Dohme and hydrogenous ethylene oxide from B.D.H. They were purified and polymerized in an identical manner. After it was degassed by repeated freezing, evacuating to 10^{-4} Pa, and thawing, the monomer was distilled on to a fresh sodium mirror in a round-bottomed flask attached to the high-vacuum line. Complete removal of the impurities necessitated the distillation of the monomer onto a further three fresh sodium mirrors. The ethylene oxide was then distilled into an evacuated flask fitted with a septum and containing a few crystals of fluorene. On thawing the monomer a small volume of *n*-butyllithium was injected through the septum. The fluorene anions generated ensured the complete removal of all polar impurities. This was essential for successful polymerization. Following the prepolymerization step, the required volume of ethylene oxide was distilled into an evacuated flask, into which was also distilled a known volume of pure tetrahydrofuran (THF). The flask was then sealed and removed from the vacuum line. After flask and contents were cooled to 195 K, polymerization was initiated by injecting a solution of diphenylmethylpotassium in THF. The flask and contents were then warmed up to room temperature over a period of 12 h and held at 340–345 K for 4 days. The reaction was "killed" by addition of a small volume of glacial acetic acid and the polymer precipitated by slow addition of the THF solutions to vigorously stirred *n*-hexane. After it had been removed by filtration the polymer was dried under vacuum at room temperature.

The number-average molecular weights were obtained by membrane osmometry (Knauer Osmometer) of solutions in 1,2-dichlorobenzene at 310 K. Weight-average molecular weights were determined by low-angle laser light scattering from solutions in the same solvent, using a Chromatix KMX-6 photometer. For the calculation of M_w, an independent measurement of the specific refractive index increment at 633 nm of PEO in 1,2-dichlorobenzene was made. It was found to be −0.063 mL g^{-1} at 298 K. The resulting values of the molecular weights were, for M_n and M_w respectively 15.8 × 10^3 and 19.2 × 10^3 for PEO-*h* and 19.6 × 10^3 and 22.1 × 10^3 for PEO-*d*.

Theory

Specular Reflection of Neutrons. Neutrons are specularly reflected in the same way as light polarized perpendicular to the plane of reflection. The reasons for this are discussed in detail by Lekner.[12] Thus any method that has been used for calculating optical reflectivites can be applied to the reflection of neutrons. In this paper we generally use the optical matrix method[13] in which the surface region is divided into a chosen number of layers whose refractive indices are calculated from the composition according to eq 1 and 2. The Fresnel reflection and transmission coefficients are calculated for each layer by using the appropriate values of the refractive indices[13] and then combined to give the characteristic reflectivity matrix, from which the reflectivity of the surface is obtained. The method lends itself to machine solution and for the types of system studied here there is no practical restriction on the number of elements into which the interface may be divided.

The advantage of neutrons or X-rays over light is that the refractive index is simply related to composition. For neutrons

$$\eta = 1 - (\lambda^2/2\pi)\rho_s \tag{1}$$

where ρ_s is the scattering length density given by

$$\rho_s = \sum n_i b_i \tag{2}$$

where n_i is the number density and b_i the experimentally determined scattering length of the nucleus i. Thus, by use of the optical matrix method, the reflectivity profile

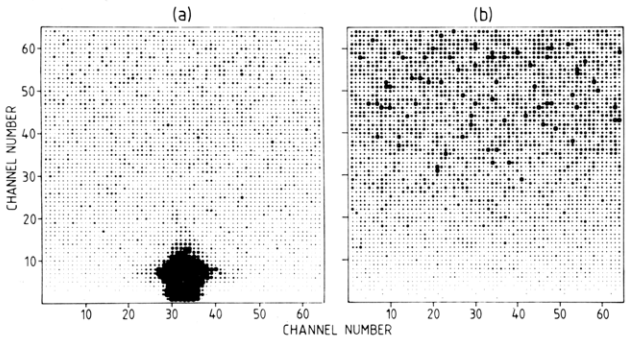

Figure 2. Neutron scattering patterns registered on the multidetector for (a) D_2O and (b) water contrast matched to air (0.088 mol fraction of D_2O). λ = 12 Å and momentum transfer = 0.036 Å^{-1}. Only the central 64 channels of the multidetector are shown. The dots in increasing order of size represent intensities in 0–100 intervals between 0 and 800. The completely filled points represent intensities greater than 800. The specular peak of D_2O reaches a maximum value of 244 000.

can be calculated exactly for any given model of the interfacial composition. The relation between these two quantities is complicated and it is not easy to assess whether it is unique, especially where the interfacial profile is itself complicated. This question is discussed further in the analysis of the results.

An alternative theoretical approach is the kinematic (first Born) approximation which gives the following expression for the reflectivity

$$R = 16\pi^2 m h(\kappa)/\kappa^2 \quad (3)$$

where m is the excess scattering length density integrated over the interfacial region (the zeroth moment of the distribution), κ is the momentum transfer normal to the interface ($\kappa = 4\pi \sin\theta/\lambda$), and $h(\kappa)$ is the form factor of the interface.[15] The form factor is the normalized modulus of the Fourier transform of the scattering length density profile of the solute across the interface

$$h(\kappa) = |\rho(\kappa)|^2/|\rho(0)|^2 \quad (4)$$

The momentum transfer covered in these experiments corresponds to the range of the initial decay of the form factor. The change in reflectivity with momentum transfer is more rapid the thicker the layer.

An important feature of the specular reflection of neutrons is that the scattering lengths of deuterium and hydrogen, and as a consequence the scattering length densities of D_2O and H_2O, are of opposite sign. It is therefore possible to make an H_2O/D_2O mixture which has the same scattering length density as air and therefore gives no specular reflection at any angle (see Figure 2). The molar ratio of D_2O to H_2O in this mixture is 0.088. We will refer to it as contrast-matched water. At low concentrations of solute in contrast-matched water, such as used in these experiments, the contrast of the bulk solution remains sufficiently close to that of air for there to be negligible specular reflection unless the solute is adsorbed at the surface. Thus the reflectivity depends only on the solute profile at the surface. In practice, the situation is slightly less simple in that there is a background because of the large incoherent scattering cross section of protons. However, incoherent scattering is approximately isotropic and is therefore distributed over a large solid angle, in contrast to specular reflection. In the region of the specular peak the relative contribution of the incoherent scattering is very small. This is discussed further below. As well as being able to examine the solute profile independently of the solvent, we were able to measure just the solvent profile by matching the scattering length density of the solute to that of air. This is achieved approximately by using the fully protonated polymer in D_2O.

The large difference in scattering length of H and D also gives neutrons a distinct advantage over X-rays for this experiment. It will be shown below that the adsorbed layer is a mixture of PEO and water but with water the dominant component. The difference in the X-ray scattering lengths of PEO and water is small and, when the composition of the adsorbed layer is taken into account, the contrast between the interfacial and bulk regions becomes very small indeed. Furthermore, the sensitivity of the X-ray experiment to the adsorbed layer cannot be enhanced by contrast matching the bulk solution to air.

The specularly reflected beam only falls on a very small number of channels of the multidetector. Incoherent scattering and small-angle scattering from the bulk polymer solution are spread over a large part of the detector. Since neither of these types of scattering has been studied in grazing incidence geometry and since they both contribute to background scattering in the region of the specular beam, we here consider their effect on the results. Figure 2 shows the patterns obtained on part of the multidetector for D_2O and contrast-matched water. They are normalized to the incident flux and plotted on the same scale. The specular peak is several orders of magnitude larger than the general level of the background. In the region of the specular peak the background is similar for D_2O and contrast-matched water. At first sight, this is somewhat surprising since the incoherent scattering cross section of contrast-matched water is more than an order of magnitude greater than that of D_2O. The effect of grazing incidence is, however, that the neutron beam is entirely scattered by much less than the first millimeter of the horizontal liquid sample, even if the cross section of the sample is small. Thus for both D_2O and H_2O the whole beam is eventually scattered, although by quite different depths of material. Detailed examination by Monte Carlo simulation shows that there are differences at higher angles and at shorter wavelengths.[14] For example, near the top of the detector the intensity from contrast-matched water is much greater than from D_2O and this is predicted by simulations. For the purposes of this paper, Figure 2 shows that the specular reflectivity can be obtained accurately by summing the counts over the appropriate area of the detector and subtracting the corresponding sum obtained from contrast-matched water.

Results

Amount of Polymer Adsorbed: Comparison with Experiment. The reflectivity of deuterated polyethylene oxide (PEO-*d*) in contrast-matched water was measured at three concentrations, 0.1%, 0.02%, and 0.004% by weight of PEO, at a temperature of 294 K. As explained in the previous section, any specular reflection from these solutions results only from PEO adsorbed at the surface. The reflectivities after subtraction of the background are shown in Figure 3a.

The reflectivity changes with concentration in two ways. There is a small drop in the overall level on going from the 0.1% to the 0.02% solution and there is also a change in the slope of the profile. We deduce from the change in slopes in Figure 3 for the two solutions 0.1% and 0.02% that the adsorbed PEO layer is thinner at the lower concentration. The general level of reflectivity is largely determined by the total scattering length density in the layer. This is clear from the kinematic theory (eq 3 and 4) where m is the integrated scattering length density over the interface which determines the overall level of reflectivity. Thus the slightly decreased reflectivity of the 0.02% so-

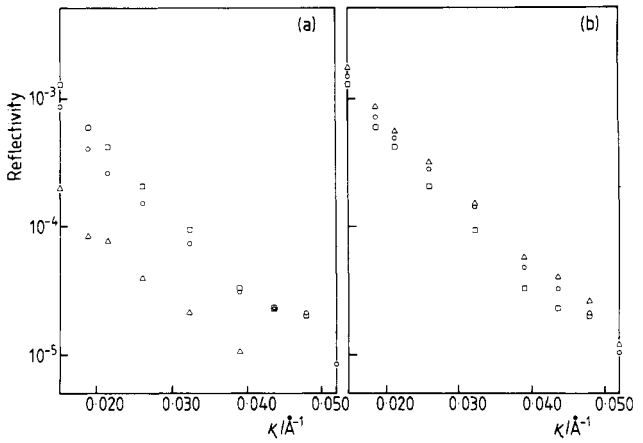

Figure 3. Specular reflection profiles obtained for solutions of deuterated poly(ethylene oxide) in contrast-matched water: (a) PEO-*d* concentrations are 0.004% (△), 0.02% (○), and 0.1% by weight (□); (b) PEO-*d* concentration is 0.1% at temperatures of 294 (□), 308 (○), and 347 K (△). Error bars have been omitted for clarity. They are shown in subsequent diagrams.

lution corresponds to a decrease in the amount adsorbed. There is a much larger drop in reflectivity for the 0.004% solution, but no change in the slope, indicating that the dimensions of the layer are the same as at 0.02% but that the amount adsorbed has decreased substantially.

It is interesting to compare these measurements with the earlier isotherm measurements of Glass[3] and with the more recent Π–*A* measurements.[4-6] For these purposes we compare the data with the calculated profiles for the simple model of a single layer of adsorbed PEO of uniform composition. Although this is not a realistic model, it is usually sufficient to characterize approximately the thickness and amount of adsorbed material.[16] However, if there is a significant contribution from segments deep in the solution their contrast will not be enough to contribute to the signal. The procedure may then underestimate the amount adsorbed. The values of the two parameters, amount and thickness, are derived by doing a full optical matrix calculation of the reflectivity and obtaining a best fit to the data. Defining a "best fit" for this type of data is not easy. This problem is discussed in ref 16 and, in particular, is illustrated in Figure 2 of that paper. It is interesting to note at this stage that this simple model does not fit the data well (see Figure 6a). We return to a discussion of this point below. The resulting values of thickness, *t*, area per monomer at the surface, and scattering length density are given in Table I.

The measurement of adsorption most directly obtained from the experiment is the area occupied per monomer unit, A_m, which is derived by dividing the scattering length of a segment (4.58×10^{-4} Å) by the product of the observed scattering length density and thickness of the layer. The scattering length densities and areas per monomer unit are given in Table I.

The variation of A_m with concentration, even for just these three concentrations, suggests that the monolayer is not complete until a concentration of at least 0.1 wt %. This disagrees with the results obtained by Glass,[3] who found for a sample of molecular weight 13 000 that the monolayer was complete at a concentration of about 0.002%. We have no definite explanation for this discrepancy, although there are two possibilities.

Glass's samples were apparently not monodisperse, although no measure of this was given, and some of them apparently contained impurities. Any organic impurity would itself be surface active in water and might act in two ways. It could lower the surface tension more than the polymer and would therefore indicate adsorption of polymer where none was occurring. If the organic material were a better solvent for the polymer than water, it could enhance the surface activity of the polymer and cause adsorption at a lower concentration. The effects of polydispersity are not as easily estimated. Glass's results show that poly(ethylene oxides) of molecular weight lower than about 10 000 are adsorbed in a lesser amount at the air–water interface but are adsorbed more rapidly. Thus one might expect a stronger final adsorption of higher molecular weight species but with some initial delay.

Table I
Parameters of the Uniform Layer Model of Adsorbed PEO

% PEO-*d*	[$MgSO_4$]	*T*/K	*t*/Å	$10^6\rho/\text{Å}^{-2}$	$A/\text{Å}^2$ monomer^{-1}
0.1		294	90 ± 5	0.45 ± 0.05	11.3 ± 1
0.02		294	80	0.40	14.3
0.004		294	80	0.20	28.6
0.1		308	90	0.55	9.3
0.1		317	90	0.58	8.8
0.1	0.4	294	90	0.58	8.8
0.1	0.4	308	90	0.65	7.8
0.1	0.4	317	90	0.75	6.8
0.02	0.4	294	90	0.47	10.8
0.02	0.4	308	90	0.55	9.3

A second possibility is that our system was not given sufficient time to come to equilibrium. Glass found that it took some time for the surface tension to reach its equilibrium value. Although not measured directly, the time constants were determined by extrapolation and equilibration times in the range of 0–12 h were found. More recently Sauer et al.[6] have determined the rate of formation of the adsorbed layer more accurately and have found shorter equilibration times in the range 0–3 h, depending on the concentration. The difference between the two measurements also suggests that Glass's samples were not monodisperse because smaller molecular weight species would first adsorb at the surface at a diffusion-controlled rate and then there would be a longer period of rearrangement as the more strongly adsorbed, larger molecular weight species gradually displaced the smaller molecules.[17] According to the values of the rates determined by Sauer et al., the equilibration times for our concentration range would be expected to be much less than 3 h. Before measurement of the reflectivity, our samples were left in the trough for 1–3 h and a set of measurements usually took from 4 to 6 h. In most cases we measured the reflectivity at one angle near the beginning of a run and again at the end but never found any difference. Furthermore, no differences were observed between reflectivities measured in the first hour of filling the trough and those measured several hours later. When the temperature was altered the substantial changes in the surface coverage seemed to keep pace with the change in temperature, also indicating that equilibration was rapid. We therefore conclude that the surfaces of our solutions had reached equilibrium.

Sauer et al.[6] have shown by light-scattering measurements that spread PEO monolayers are identical with those found by adsorptiodn from solution. We may therefore compare our values of A_m at the completed monolayer with the value of the area per monomer unit at a surface pressure just sufficient to reach the plateau of the Π–*A* isotherm. The results of both Sauer et al. and Kuzmenka and Granick[4,5] show that at 298 K the monolayer is complete when the surface excess, Γ, is between 0.65 and 0.8 mg m^{-2}, which corresponds to an area per segment in the range 11–9 Å^2. Our estimate of 11.3 ± 1

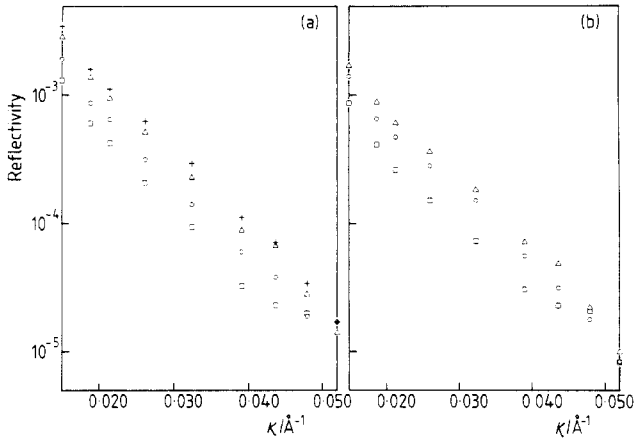

Figure 4. Effects of added 0.4 M $MgSO_4$ on the reflectivity of PEO-*d* in contrast-matched water: (a) in order of increasing reflectivity the profiles are for 0.1% PEO-*d* at 294 K with no added $MgSO_4$ (□) and for 0.1% PEO-*d* at 294 K (○), 0.1% PEO-*d* at 308 K (△), and 0.1% PEO-*d* at 317 K (+), all in 0.4 M $MgSO_4$; (b) in order of increasing reflectivity, 0.02% PEO-*d* at 294 K (□), 0.02% PEO-*d* in 0.4 M $MgSO_4$ at 294 K (○), and 0.02% PEO-*d* in 0.4 M $MgSO_4$ at 308 K (△).

$Å^2$ for the area per monomer at the completion of the monolayer is therefore in good agreement with the results from the Π–*A* isotherms. The cross-sectional area of a monomer is approximately 16 $Å^2$ so that the monolayer cannot be purely two dimensional.

The effects of increasing the temperature for the 0.1% solution are shown in Figure 3b and may also be analyzed by the simple model described above. There is a significant increase in the level of reflectivity between 294 and 317 K but no significant change in the slope of the reflectivity profile. The results of fitting the uniform layer model to the observations, shown in Table I, confirm that there is an increase in the total amount of adsorbed PEO with temperature. In terms of the area occupied per segment, there is approximately a 20% decrease on increasing the temperature from 294 to 308 K, which is again in good agreement with the Π–*A* isotherm measurements of Kuzmenka and Granick.[4] On the other hand, Glass found a zero temperature coefficient of the surface excess.

The effect of adding the electrolyte $MgSO_4$ is, as with increasing the temperature, to increase the amount of PEO adsorbed at the surface without significantly altering the thickness of the layer (Figure 4a). At 0.4 M $MgSO_4$ and 294 K the reflectivity of the 0.1% solution is almost the same as the reflectivity of the 0.1% solution without $MgSO_4$ at 317 K. The result of heating the 0.1% solution containing 0.4 M $MgSO_4$ is to increase the reflectivity. Analysis by means of the uniform layer model shows that the dimensions of the layer change negligibly but the amount adsorbed has increased. At 317 K and 0.4 M $MgSO_4$ the amount adsorbed at the surface of the 0.1% solution has almost doubled from its value in water at 294 K. Although Kuzmenka and Granick have also measured the Π–*A* isotherms in the presence of $MgSO_4$,[5] it is not possible to compare our result quantitatively because their Π–*A* isotherm has not quite reached a plateau at 7.2 $Å^2$ per segment and, in any case, their $MgSO_4$ concentration was 1 M. However, once again there is excellent semiquantitative agreement. The effect of adding salt to the 0.02% solution of PEO is to increase both the amount adsorbed and the thickness of the adsorbed layer so that it becomes similar to the 0.1% solution at 308 K (Figure 4b).

Amount of Polymer Adsorbed: Comparison with Theoretical Prediction. Water is a good solvent for PEO at 298 K but as the temperature is raised it becomes poorer, reaching the Θ point at 369 K. Over this range the polymer–solvent interaction parameter, χ, increases approximately linearly with temperature from 0.460 (at 298 K) to 0.5.[18] One of the factors determining the amount of polymer adsorbed at a surface is the difference between the adsorption parameter, χ_s, and χ.[18] When both χ and χ_s are of the same order, the amount adsorbed changes rapidly with small changes in χ_s. This is a feature of all of the main quantitative theories of polymer adsorption. If we assume that for PEO at the air–water interface χ_s is independent of temperature, we can use the known solvent parameters to predict the amount adsorbed at each temperature. To what extent this assumption can be justified is discussed further below. To cover the maximum range of variation of χ, we need to make a further assumption about χ for solutions with and without $MgSO_4$. A solution of PEO in 0.4 M $MgSO_4$ has a Θ temperature of 317 K and is therefore equivalent to PEO in water alone with a Θ temperature of 369 K. The experimental results of Table I show that the adsorption is the same for 0.4 M $MgSO_4$ at 294 K and water at 317 K and we therefore assume that χ is the same for these two solutions. Linear interpolation gives an estimate for χ of 0.488 for 0.4 M $MgSO_4$ at 308 K.

The amount of polymer adsorbed was calculated by using the Scheutjens and Fleer mean-field calculation, which is described in detail in ref 19. The number of statistical segments in a PEO molecule of molecular weight 20 000 was calculated from the characteristic ratio of PEO[20] to be 75, each segment consisting of about five monomer units with a length of 21 Å. χ_s was taken to be zero in all but the first layer. The most satisfactory fit to the overall level of the adsorption was found to be with a χ_s of about 0.43 ± 0.05. It can be seen from Figure 5a that the observed increase in the amount adsorbed as χ increases is more rapid than predicted by the mean-field calculation. This may, of course, simply be explained by an increase in the adsorption parameter χ_s with temperature and not just the increase in the polymer–solvent interaction parameter. The increase in χ_s required would be about 20% from the lowest to the highest adsorption. However, the liquid/vapor interface is quite different from the solid/liquid interface because it is less "two dimensional" and because χ_s is a free energy rather than an enthalpy. χ_s may therefore be more sensitive to changes in temperature.

The mean-field calculation predicts rather less satisfactorily the variation of amount adsorbed with change in concentration as shown in Figure 5b. The two lowest concentrations lie on the predicted curve (for $\chi_s = 0.45$ and $\chi = 0.46$), but then the amount adsorbed appears to stop increasing so rapidly; i.e., the growth of the polymer layer is complete before the segment density in the surface layer reaches a volume fraction of one. The mean-field theory predicts continuing adsorption of polymer as the concentration is raised above 0.1% by weight. Scaling law predictions also fail to account for the concentration variations in this system for similar reasons. This may be a peculiarity of the PEO–water system, which has strong specific polymer–solvent interactions, since scaling predictions account satisfactorily for the concentration variation of surface tension in the poly(dimethylsiloxane)–toluene system.[21]

Segment Density Profile of the Adsorbed Polymer Layer. There are several theoretical predictions for the segment density profile of an adsorbed polymer layer. Scaling laws have been used to predict analytical segment density profiles,[21,22] and a number of other models, mostly

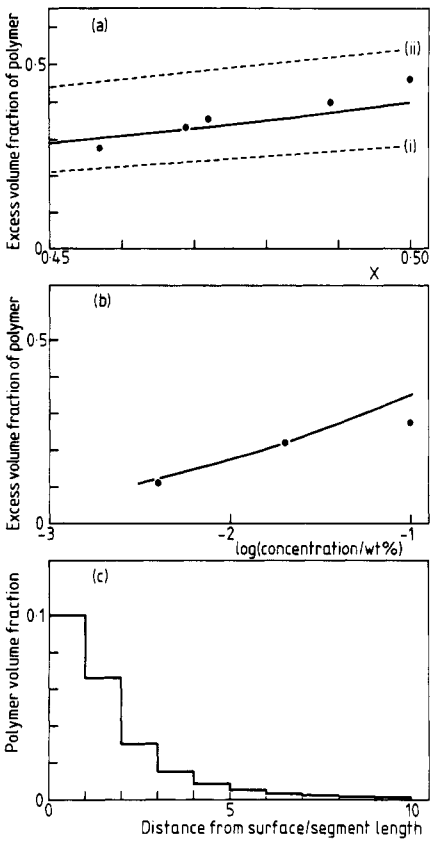

Figure 5. (a) Comparison of the total adsorption predicted by the mean-field (Scheutjens–Fleer) theory with that observed as a function of solvent parameter. The continuous line is calculated for an adsorption parameter, χ_s, of 0.43 and the dashed lines are for values of (i) 0.4 and (ii) 0.5. The number of segments is 75. (b) Comparison of the calculated and observed total adsorption as a function of concentration: $\chi = 0.46$ and $\chi_s = 0.45$. (c) The calculated segment density profile for 0.1% polymer at $\chi = 0.46$ and $\chi_s = 0.40$. The segment length for PEO is 21 Å.

only soluble numerically, have been critically assessed by Fleer and Lyklema.[23] We now consider to what extent the reflectivity profile gives information about the segment density profile.

Figure 6a shows the fit of the reflectivity calculated for a single layer of scattering density 0.45×10^{-6} Å^{-2} and thickness 90 Å to the data for 0.1% PEO-*d* in water at 294 K. Such a simple fit might suggest that the reflectivity measurement has not been extended to a high enough momentum transfer to be sensitive to the shape of the segment density profile. That this is not the case is shown by the fit in Figure 6b of the reflectivity calculated for the mean-field segment density profile obtained from the Scheutjens–Fleer calculation described in the previous section (shown in Figure 5c). The parameters used were $\chi = 0.46$ and $\chi_s = 0.4$. A value of 0.4 for χ_s was chosen rather than the 0.43 used in Figure 5a because it gave a better fit to the general level of the reflectivity. To convert the calculated segment density profile, which is a volume fraction profile, to a scattering length density, we combined the volume of a monomer segment of 65.3 Å^3, derived from the value of 1.13 for the bulk density,[24] with its scattering length. This gives a value of the scattering length density of bulk PEO-*d* of 7.01×10^{-6} Å^{-2}. Figure 6b shows that the Scheutjens–Fleer segment density profile does not account for the observed shape of the reflectivity profile. Adjustment of any of the parameters χ, χ_s, or the number of segments does not change the shape of the calculated profile significantly, it merely alters the level of reflectivity. Analysis of the problem using kinematic theory shows that the mean-field calculation predicts too little polymer at larger depths (greater than about 50 Å) and too much close the surface. The latter has the effect of increasing the reflectivity at larger momentum transfer and the former of decreasing the reflectivity at small momentum transfer. The mean-field analytical expression for the segment density profile in a good solvent is[25]

$$\phi(z) = \phi_b \coth^2\left[\frac{z + D}{\xi}\right] \tag{5}$$

where z is the depth, D is a length characterizing the strength of adsorption, and ξ the mean-field correlation length. This produces a similarly shaped reflectivity profile to that shown in Figure 6b. The scaling prediction for the segment density profile in a good solvent is[25]

$$\phi(z) = \phi_b\left[\frac{z + 4D/3}{a}\right] \tag{6}$$

where a is the length of a monomer unit. This formula only holds for that part of the profile between D and R_g. The shape of this profile is qualitatively similar to that of the mean-field profile and gives a similarly shaped reflectivity profile. Part of the difficulty could lie in the effects of the layer nearest the surface on the reflectivity. This layer is not precisely defined geometrically in either theory. For example it could be flattened or it could become more diffuse because of roughening of the surface. However, the inclusion of variations in its thickness only slightly improves the fits to the observations in the higher angle range. There remains the underestimation of the reflectivity at lower angles, which results from the contributions of segments at depths greater than about 50 Å.

Extra information is given by the reflectivity profiles of PEO-*h* in D_2O. The reflectivity of PEO-*d* in contrast-matched water depends only on the distribution of the polymer segments at the surface. The profile of PEO-*h* in D_2O is in contrast largely determined by the profile of

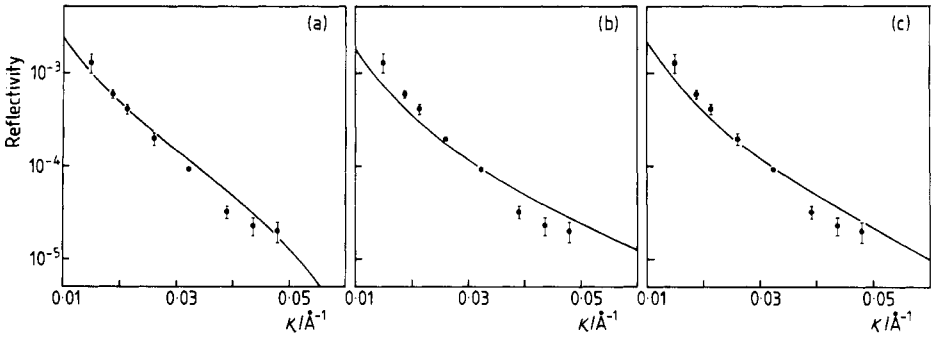

Figure 6. Fit of calculated reflectivity profiles to 0.1% dPEO in null water at 294 K: (a) single layer, thickness 90 Å and scattering length density 0.45×10^{-6} Å^{-2}; (b) the mean-field profile shown in Figure 5b; (c) the mean-field reflectivity profile with adsorption parameter of 0.18 for the first and second layers.

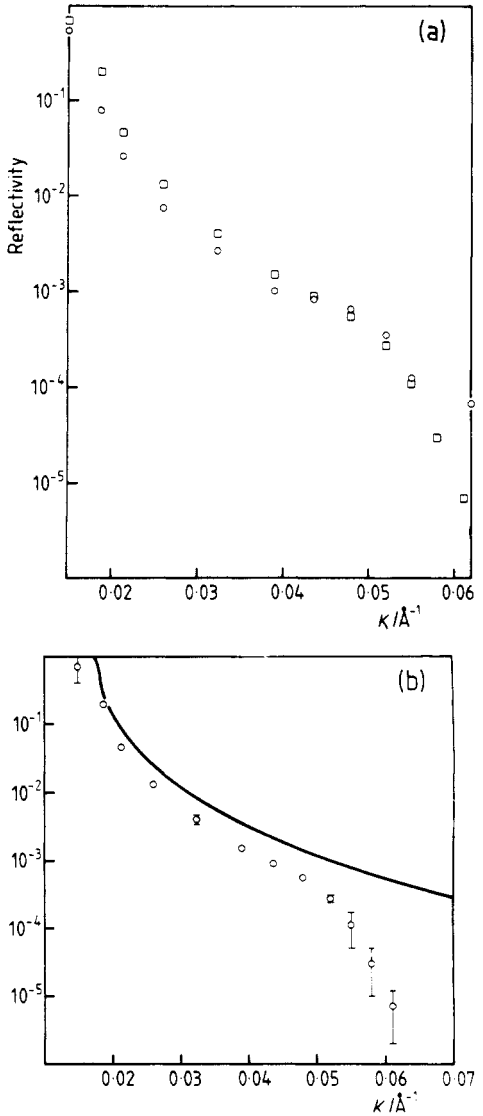

Figure 7. (a) Reflectivity profiles of 0.1% by weight of PEO-*h* in D_2O at 294 (□) and 318 K (○). The higher temperature run consists of the results at both 308 and 318 K. Where these overlapped there was no observable difference. (b) Comparison of the profile for 0.1% PEO-*h* in D_2O at 294 K with that calculated for perfectly smooth D_2O.

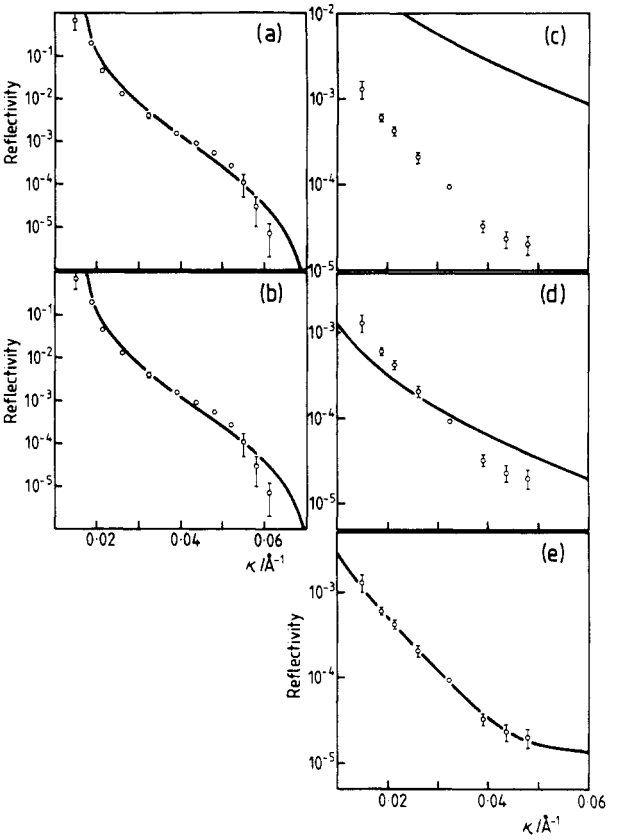

Figure 8. Comparison of calculated and observed reflectivity profiles: (a) 0.1% PEO-*h*/D_2O with a model of a single layer with a thickness of 45 Å and a scattering length density of 3.2×10^{-6} Å^{-2} (scattering length density of D_2O is 6.38×10^{-6} Å^{-2}); (b) 0.1% PEO-*h*/D_2O with a two-layer model, scattering length densities 3.2×10^{-6} and 6.2×10^{-6} Å^{-2}, respectively; (c) 0.1% PEO-*d*/contrast-matched water with a model of a single layer with a thickness of 45 Å and a scattering length density of 4.2×10^{-6} Å^{-2}; (d) 0.1% PEO-*d*/contrast-matched water with a model of a single layer with a thickness of 45 Å and a scattering length density of 0.65×10^{-6} Å^{-2}; (e) 0.1% PEO-*d*/contrast-matched water with a two layer model, thicknesses 45 and 80 Å and scattering length densities 0.65×10^{-6} and 0.2×10^{-6} Å^2, respectively. Temperature = 294 K throughout.

the D_2O at the surface because the scattering length density of bulk PEO-*h* (0.68×10^{-6} Å^{-2}) is small in comparison with that of D_2O (6.38×10^{-6} Å^{-2}). However, if PEO is adsorbed at the surface it will exclude solvent and the depletion layer of the solvent should be related to the segment density profile of the polymer. Depletion of solvent from the surface will generally lower the reflectivity. The results for PEO-*h* in D_2O are shown in Figure 7a for 0.1% by weight of PEO-*h* in D_2O at two of the temperatures used for the deuterated polymer in contrast-matched water. The reflectivity is considerably depressed from its value for pure D_2O (Figure 7b).

Given the similarity in the molecular weights of the two PEO samples, it is reasonable to assume that the structures of the adsorbed layers in the two isotopic systems are identical (only small differences are found in the bulk phase diagram[26]). Any structural model must therefore fit both sets of data in Figure 7 and Figure 3b. We now attempt to do this for the 0.1% sample at 294 K.

There is a dip in the reflectivity profile for PEO-*h* in D_2O at a κ of about 0.065 Å^{-1}. This is what would be expected for a single layer 35–55 Å thick with a scattering length density about half that of D_2O. The best fit of such a model to the data is shown in Figure 8a and has a layer thickness of 45 ± 10 Å and a scattering length density of $3.2 \pm 0.5 \times 10^{-5}$ Å^{-2}. If we now assume that PEO and D_2O retain their bulk densities in the surface layer, we can calculate the volume fraction of PEO in the surface region and hence show that the corresponding scattering length density for PEO-*d* in contrast-matched water will be 4.2×10^{-6} Å^{-2}. The reflectivity profile of a 45-Å layer of this scattering length density on contrast matched water is shown in Figure 8c. It does not fit the data for the equivalent PEO-*d* solution.

It has already been shown that the PEO-*d* data are in excellent agreement with Π–*A* measurements. Thus the measurements on PEO-*h* in D_2O are overestimating the fraction of low scattering length matter in the surface region. In the model of the previous paragraph we have assumed that the low scattering matter is all PEO. This cannot be consistent with either the PEO-*d* measurements or the separate Π–*A* measurements. Apart from possible defects in the experimentation or unusually large isotope effects leading to a difference in chemical structure, both of which we will examine further below, the only way to reconcile the two sets of data is if a significant proportion of the low scattering matter in the surface layer is air. The two sets of data can then be approximately explained by a single structural model if the 45-Å layer contains 9% by

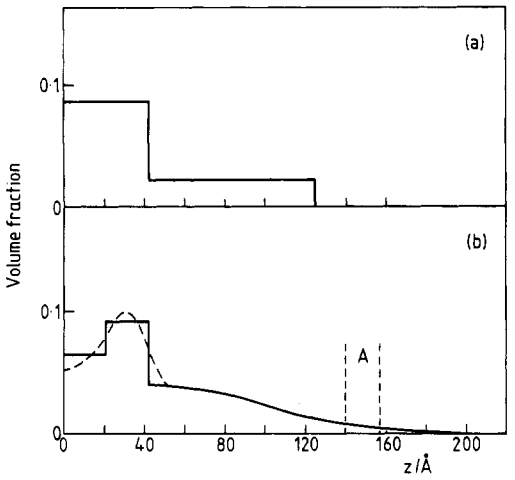

Figure 9. Segment density profiles for 0.1% PEO in water: (a) the simplest model that fits the observations at 294 K; (b) an equivalent two-layer model in the interfacial region and a half-Gaussian distribution of the loops and tails. The dashed line represents a smoother distribution, which would also fit the data.

volume of polymer, 50% D_2O, and 41% air. Figure 8a,d compares the calculated and observed profiles for such a surface layer. Although the D_2O data are fitted approximately (Figure 8a), the model still does not account for the shape of the reflectivity profile of PEO-*d* (Figure 8d). The inclusion of a second deeper layer that contains about 2.5% PEO and is about 80 Å thick greatly improves the fit to the PEO-*d* profile (Figure 8e), while making only very slight differences to the PEO-*h* profile (Figure 8b). The value of the area per monomer segment is slightly changed from the single layer model and is 9.9 Å^2, corresponding to a surface excess of 0.7 mg m^{-2}, which agrees almost exactly with the value for the completed monolayer in the Π–*A* isotherms.[4-6] The volume fraction profile of the polymer is now as shown in Figure 9a.

Discussion

To fit the two sets of isotopic data with a single structural model, it is necessary to invoke the presence of air in the surface region. The need to include air in the layer nearest the surface in order to reconcile measurements on different isotopes was also found in the treatment of surface layers[16] and presumably arises from some kind of roughening of the surface by the polymer. The polymer loses configurational entropy when it is adsorbed at the surface but this effect will be reduced if the polymer can fluctuate through the interface. Hone et al.[27] have shown that the effect of a rough surface is to enhance the amount adsorbed, mainly because of an increase in the available surface area. Here we have a rather different effect in that there must be some cooperativity between roughening of the surface and increased adsorption. If roughening of the surface does occur, the thickness of the rough layer would be expected to be comparable with the statistical segment length. Since this is only 21 Å and the thickness of the surface region is 45 Å, it seems likely that the surface is further divided into two regions with the one nearest the surface containing a larger fraction of air and correspondingly smaller fractions of both polymer and water. Such a division will still fit the observed reflectivities within certain limits, provided that the deeper 80-Å layer needed to fit the data in Figure 8e is retained. Thus the data can be fitted by an upper layer containing about 40% and a lower layer containing about 70% by volume of polymer plus water.

The presence of a rough interface between a polymer solution and air has not previously been suggested. Kawaguchi et al.[7] have used ellipsometry to study the surface of PEO solutions but did not observe any roughness. However, the optical refractive index contrast is very low between water and PEO and the best that can be done with ellipsometry is to test the consistency of different structural models with the data. Kawaguchi et al. had particular difficulty in reconciling their ellipsometric and Π–*A* determinations for the amount of PEO adsorbed, let alone in determining a unique structural model. Thus, although their measurements give no support to our results, neither do they necessarily contradict them.

The anomalous data that require the introduction of the rough interfacial model would seem to be the measurements on the PEO-*h* in D_2O since the PEO-*d* measurements are in excellent agreement with Π–*A* curves. We now examine other possible explanations for the anomalous reflectivity of the PEO-*h* solutions. The first possibility is contamination by surface-active impurities in the solution. Any such impurities will be proton containing and could exert a large effect on the reflectivity from D_2O. However, although they would have no effect on the reflectivity from the null scattering solutions, such impurities would have caused anomalous adsorption of PEO-*d*. The good agreement of the PEO-*d* data with the Π–*A* isotherms indicates that the contrast-matched water solutions were clean. Since the solutions of PEO-*h* in D_2O were prepared identically, it is unlikely that they were at all contaminated. The second possibility is that there is a large isotope effect. This might be possible near the cloud point but is unlikely at 294 K because the bulk equilibria show only small isotope effects.[26]

In comparison with a polymer layer adsorbed at a flat wall, the segments in the 45 Å layer must be regarded as the adsorbed trains, although they have some looplike characteristics. The remainder of the polymer extending into the solvent consists of loops and tails. The model of a uniform layer for this region is therefore physically unrealistic and we have attempted to fit a number of other shapes for the segment density profile. For example, we can now repeat the Scheutjens–Fleer calculation, taking into account the rough surface. This can be done by allowing specific adsorption to occur into both first and second layers. Figure 6c shows the results of such a calculation where the polymer–solvent interaction parameter has been given the observed value of 0.46 and χ_s for the first and second layers is taken to be 0.2. This gives the correct total amount adsorbed but with polymer volume fractions of 0.06 and 0.09 in the first and second layers, respectively. The figure shows that, once again, the mean-field calculation does not predict enough polymer in the loop and tail region to account for the observed reflectivity profile. The calculated distribution falls off too rapidly to account for the observations. This is also found to be the case for linear and exponential decays. The only simple distribution to fit the data is a half-Gaussian, $A \exp(-z^2/L^2)$, with $A = 0.26$ and $L = 80$ Å. A segment density profile consisting of a roughened surface and a Gaussian decay of the loop and tail region is shown in Figure 9b. This is physically more realistic than the two-layer model shown in Figure 9a, but it should be emphasized that the experiment does not distinguish the two at this resolution.

Table I shows that the effect of increasing χ is to increase the surface excess of PEO. It is not possible to show how the segment density profile changes for most of the conditions given in the table because the reflectivity profiles of both PEO-*d* in contrast-matched water and PEO-*h* in D_2O are required to distinguish the two scattering

blocks. However, we are able to do the calculation for PEO in water at 318 K. The PEO-h/D_2O profile changes significantly with the change in temperature, as shown in Figure 7a. At the higher temperature the reflectivity is lower at small κ and higher at large κ. This indicates that there is more PEO in the loop and tail region and that the 45-Å layer at the surface is less distinct. In conjunction with the PEO-d/null water results and the assumption that the loop and tail region decays as a half-Gaussian, we obtain a segment density profile similar to that of Figure 9b but with a thicker surface layer and more PEO in the loop and tail region. However, there is no change in the decay length of this region.

In the kinematic approximation, the reflectivity can be thought of as depending approximately on $h(\kappa)$, and since this is the squared Fourier transform of the inhomogeneity at the interface, there is a loss of phase information that makes it impossible in principle to obtain a unique structure of the interfacial region. This problem can largely be overcome by suitable isotopic substitution and by the physical reasonableness of the result. The crude model, shown in Figure 9a, is the only reasonable one that will fit the two sets of isotopic data. However, polymer distributions are generally expected to be less abrupt and the model shown in Figure 9b is more physically reasonable and yet still consistent with the data. However, the extra number of layers that have now been included introduce new problems of uniqueness. For example, it would be possible to fit the data adequately with changes within the first three layers. For this reason we have drawn a smooth profile through the model shown in Figure 9b. This would not be a radical revision of the model but would be quantitatively different. To obtain the finer detail it would be necessary to measure the reflectivity profile to a higher value of the momentum transfer. Measurements on a much higher molecular weight polymer would also make it easier to measure the segment density profile over a larger relative distance.

It is interesting to compare the reflectivity experiment with neutron small-angle scattering experiments. A discussion of the latter has been given in ref 28. The experiment depends on contrast matching a colloidal particle to the solvent and then measuring the scattering from the polymer layer. In principle, this may contain scattering from the structure normal to the surface (interference) and from the in-plane structure (diffuse).[29] There are three differences from the reflection experiment. First, exact contrast match may be difficult to achieve because the composition and density of the colloidal particle are not easy to establish to the precision needed. In reflection experiments contrast matching to remove the solvent contribution is simple. Second, specular reflection depends only on the mean composition profile normal to the surface. Fluctuations, especially in the plane of the surface, give rise to nonspecular reflection. The two are easy to separate experimentally. Indeed, we have recently measured the nonspecular reflection from a spread polymer layer and found it to be extremely weak.[30] Finally, the momentum transfers reached in a small-angle scattering experiment are often smaller than in reflection experiments, making it a lower resolution technique. For example, the maximum momentum transfer reached in ref 28 was 0.045 $Å^{-1}$. The maximum value in the present experiments (Figure 7) was 0.062 $Å^{-1}$. The reason that reflection can be done at higher momentum transfers is that the signal in the reflection experiment is highly directed. It is possible to reach momentum transfers of 0.25 $Å^{-1}$ in experiments on surfactants[16] and expected experimental improvements may extend this to 0.4–0.5 $Å^{-1}$.

The segment density profile of Figure 9b qualitatively resembles profiles that have been calculated for weak adsorption.[31,32] Such a shape should have overall dimensions comparable to the radius of gyration. Vennemann et al.[24] have measured the radius of gyration of a monodisperse sample of PEO (molecular weight 19K, $M_w/M_n \simeq 1.1$) in water. Their value for $\langle R_g^2 \rangle^{1/2}$ was 73 Å at 298 K. This compares well with our value of 80 Å for the loop and tail region of the polymer and suggests that the segment distribution in this region is quite similar to that in the unperturbed polymer.

The difficulty in fitting the mean-field calculations to the data seems to be that the segment density profile is characteristic of very weak adsorption but the total amount adsorbed indicates stronger adsorption. That mean-field and scaling predictions of the segment density fail to account for the observations may have three possible causes. First, the molecular weight of the PEO is low and may be too small to be adequately accounted for by these theories. Second, PEO in water is known to be a "peculiar" system in that the interaction between the monomer segments and solvents is highly specific. Finally, the air/liquid surface is significantly different from the solid/liquid interface, for which most of the theoretical treatments have been formulated.

It is interesting to compare the thickness of our PEO layers with the onset of steric repulsion between mica plates with adsorbed PEO. Klein and Luckham[33] found that the onset of repulsion after equilibrium adsorption of a 40 000 molecular weight sample was about 350–400 Å. We assume that the boundary layer is comparable in dimensions with PEO at the air/liquid interface and is independent of polymer size. We then subtract this thickness (90 Å) from their interaction distance, divide by $2^{1/2}$ to allow for the reduction in R_g for our polymer, and add in the boundary layer thickness once more. This would give an equivalent interaction distance of 280–310 Å. This would correspond to the onset of repulsion when the region A (see Figure 9b) of the polymer on each plate came into contact. The volume fraction here is about 0.04 so the total for the two molecules would be about 0.08. This would imply that there had to be significant overlap before steric repulsion acts.

Registry No. PEO, 25322-68-3; $MgSO_4$, 7487-88-9; neutron, 12586-31-1.

References and Notes

(1) Hayter, J. B.; Highfield, R. R.; Pullman, B. J.; Thomas, R. K.; McMullen, A. I.; Penfold, J. *J. Chem. Soc., Faraday Trans. 1* **1981**, *77*, 1437.
(2) Bradley, J. E.; Lee, E. M.; Thomas, R. K.; Willatt, A. J.; Gregory, D. P.; Penfold, J.; Ward, R. C.; Waschkowski, W. *Langmuir* **1988**, *4*, 821.
(3) Glass, J. E. *J. Phys. Chem.* **1968**, *72*, 4459.
(4) Kuzmenka, D.; Granick, S. *Macromolecules* **1988**, *21*, 779.
(5) Kuzmenka, D. J.; Granick, S. *Polym. Commun.* **1987**, *29*, 64.
(6) Sauer, B. B.; Griffin, W. G.; Yu, H. *Macromolecules*, in press.
(7) Kawaguchi, M.; Tohyama, M.; Mutoh, Y.; Takahashi, A. *Langmuir* **1988**, *4*, 407.
(8) Sansone, M.; Rondelez, F.; Peiffer, D. G.; Pincus, P.; Kim, M. W.; Eisenberger, P. M. *Phys. Rev. Lett.* **1985**, *54*, 1039.
(9) Lee, E. M.; Simister, E. A.; Thomas, R. K. *Molecular Crystals and Liquid Crystals*; in press.
(10) Neutron Facilities at the High Flux Reactor, Institut Laue-Langevin, Grenoble, 1986.
(11) Mezei, F. *Commun. Phys.* **1976**, *1*, 81.
(12) Lekner, J. *Theory of Reflection*; Martinus Nijhoff: Dordrecht, 1987.
(13) Born, M.; Wolf, E. In *Principles of Optics*, 5th ed.; Pergamon Press: Oxford, 1975; pp 51–72.
(14) Lee, E. M. Ph.D. Thesis, Oxford, 1989.
(15) Crowley, T. L.; Thomas, R. K.; Willatt, A. J., unpublished results.

(16) Lee, E. M.; Thomas, R. K.; Penfold, J.; Ward, R. C. *J. Phys. Chem.* **1989**, *93*, 381.
(17) Cohen Stuart, M. A.; Cosgrove, T.; Vincent, B. *Adv. Colloid Interface Sci.* **1986**, *24*, 143.
(18) Gregory, P.; Huglin, M. B. *Makromol. Chem.* **1986**, *187*, 1745.7.
(19) Scheutjens, J. M. H. M.; Fleer, G. J. *J. Phys. Chem.* **1980**, *84*, 178.
(20) Napper, D. H. *Polymeric Stabilization of Colloidal Dispersions*: Academic Press: London, 1983.
(21) Ober, R.; Paz, L.; Taupin, C.; Pincus, P.; Boileau, S. *Macromolecules* **1983**, *16*, 50.
(22) de Gennes, P.-G.; Pincus, P. *J. Phys.* (Les Ulis, Fr.) **1983**, *44*, L-241.
(23) Fleer, G. J.; Lyklema, J. In *Adsorption from Solution at the Solid/Liquid Interface*; Parfitt, G. D., Rochester, C. H., Eds.; Academic Press: London, 1983.
(24) Vennemann, N.; Lechner, M. D.; Oberthur, R. C. *Polymer* **1987**, *28*, 1738.
(25) Rondelez, F.; Ausserre, D.; Hervet, H. *Annu. Rev. Phys. Chem.* **1987**, *38*, 317.
(26) Richards, R. W., unpublished work.
(27) Hone, D.; Ji, H.; Pincus, P. A. *Macromolecules* **1987**, *20*, 2543.
(28) Cosgrove, T.; Heath, T. G.; Ryan, K.; Crowley, T. L. *Macromolecules* **1987**, *20*, 2879.
(29) Auvray, L.; de Gennes, P. G. *Europhys. Lett.* **1986**, *2*, 647.
(30) Rennie, A. R.; Lee, E. M.; Thomas, R. K.; Qureshi, S.; Richards, R. W.; Roberts, S.; Crowley, T. L., unpublished work.
(31) de Gennes, P.-G. *Scaling Concepts in Polymer Physics*; Cornell University Press: Ithaca, NY.
(32) Dickinson, E.; Lal, M. *Adv. Mol. Rel. Int. Processes* **1980**, *17*, 1.
(33) Klein, J.; Luckham, P. *Nature* (*London*) **1982**, *300*, 429.

Structural Studies of Polymers with Hydrophilic Spacer Groups. 2. Infrared Spectroscopy of Langmuir–Blodgett Multilayers of Polymers with Fluorocarbon Side Chains at Ambient and Elevated Temperatures

J. Schneider, C. Erdelen, and H. Ringsdorf

University of Mainz, D-6500, Mainz, Federal Republic of Germany

J. F. Rabolt*

IBM Research Division, Almaden Research Center, 650 Harry Road, San Jose, California 95120-6099. *Received October 20, 1988; Revised Manuscript Received January 31, 1989*

ABSTRACT: Multilayered Langmuir–Blodgett films of preformed polymers containing fluorocarbon side chains and hydrophilic spacer groups in the main chain have been investigated by IR spectroscopy. Grazing incident reflection and transmission measurements have been utilized to obtain information on the orientation of the side chains at room temperature and at elevated temperatures. Results indicate that the side chain is tilted relative to the surface normal unlike their hydrocarbon analogues, which are perpendicular to the surface. Although this angle of tilt increases at higher temperatures, it is shown that the initial orientation of the side chains returns when the film is cooled to ambient. This is found to be true even for temperatures as high as 150 °C in the homopolymer and 180 °C in the $m = 5$ copolymer, indicating that the main-chain spacer plays a major role in the high-temperature stability of these materials. The contribution of the rigid fluorocarbon side chain in this inherent thermal stability is discussed.

Introduction

Although much of the interest in Langmuir–Blodgett (LB) films has been in amphiphilic molecules containing hydrocarbon chains, there is an increasing realization that chemical modification of the long-chain amphiphiles so as to contain other structures can lead to novel surface properties.[1-4] Of recent interest has been the incorporation of CF_2 sequences into the structure of these lipidlike structures[5-8] with the result that liposomes, monolayers, and multilayers have all since been studied. Although the surface properties changed, no significant enhancement of the thermal and mechanical integrity was observed.

In an attempt to further improve the long-term thermal stability of LB films, the polymerization of a series of perfluorocarbon molecules containing reactive groups was investigated and compared[9] to that of their hydrocarbon analogues. An alternative approach[10] was more recently initiated to introduce polymeric properties into LB layers by the formation of a complex of a perfluorinated lipid and a polyelectrolyte counterion. Both methods found that the LB films exhibited increased stability, but their behavior at elevated temperatures was not explicitly addressed.

In general, reports of LB films of preformed polymers with fluorocarbon side chains are rare. An initial attempt[11] was made to create such novel structures by attaching perfluorocarbon chains to a polymer backbone containing random reaction sites. The nature of such a reaction is such that a random copolymer is produced. In another method, free-radical polymerization of reactive monomers containing fluorocarbon side chains was shown[12] to be successful. With this synthetic approach both a homopolymer and a series of copolymers containing varying amounts of hydrophilic comonomer units resulted. It is this set of polymers that are the subject of an IR investigation in this work. Grazing incident reflection and standard transmission measurements have been obtained on the homopolymer ($m = 0$) and two of the copolymers ($m = 1, 5$; see Figure 1) at ambient and elevated temperatures. The extent of orientation of the fluorocarbon side chain was specifically addressed as a function of backbone spacer length and sample temperature.

Experimental Section

Synthesis. The homopolymer and the copolymer $m = 1, 5, 10$ (Figure 1) were synthesized by radical polymerization in solution. A lipid monomer 1*H*,1*H*,2*H*,2*H*-perfluorodecyl methacrylate and a hydrophilic comonomer 2-HEA (2-hydroxyethyl acrylate) were used.

The polymerizations were performed in dry trifluorotoluene in the case of the homopolymer and in dry dioxane in the case of the copolymers. As initiators, 5 mol % of TBPIPC (*tert*-bu-

0024-9297/89/2222-3475$01.50/0